



Kingdom of Saudi Arabia  
Imam Mohammad bin Saud Islamic  
University College of Science  
Chemistry Department



**One pot preparation of  $\text{MoO}_3$  doped  $\text{MgOSiO}_2$  triple composites for fast removal of antibiotics from water**

*Research submitted as partial fulfillment of the requirements for the completion of the BSc Degree in Chemistry*

By

**Abdullah Mohammed Abdullah Alzahiry (442016907)**

&

**Murdi Yahya Murdi Alzahrani (442018736)**

&

**YASSER GHUSN MOHAMMED ALGHUSN (441015450)**

**Supervisor**

**Dr. Faisal K. Algethami.**

**Dr. Babiker Y. Abdulkhair**

**February - 2025**

## ***Acknowledgement & Dedication***

***Our heartfelt gratitude goes to our supervisors, for all of their help and guidance.***

***Please accept our heartfelt gratitude for the chemistry faculty's hard work.***

***This endeavor is in honor of our loved ones, who have always supported us and inspired us to keep going.***

<b><u>No.</u></b>	<b><u>Contents</u></b>	<b><u>Page No.</u></b>
	<b>Abstract (English)</b>	<b>5</b>
	<b>Abstract (Arabic)</b>	<b>6</b>
<b><u>Chapter 1</u></b>		
<b><u>Introduction and literature review</u></b>		
<b>1</b>	<b>Introduction</b>	<b>8</b>
<b>1.1</b>	<b>Preparation of nanomaterials</b>	<b>8</b>
<b>1.2</b>	<b>Common approaches for making nanomaterials</b>	<b>11</b>
<b>1.3</b>	<b>Aim of the study</b>	<b>13</b>
<b><u>Chapter 2</u></b>		
<b><u>Materials and methods</u></b>		
<b>2</b>	<b>Materials and methods</b>	<b>16</b>
<b>2.1</b>	<b>Materials</b>	<b>16</b>
<b>2.2</b>	<b>Preparation of MgSi- nanocomposites</b>	<b>16</b>
<b>2.3</b>	<b>Preparation of CF solution</b>	<b>16</b>
<b>2.4</b>	<b>CF Adsorption</b>	<b>17</b>
<b><u>Chapter 3</u></b>		
<b><u>Results and discussion</u></b>		
<b>3</b>	<b>Results and discussion</b>	<b>18</b>
<b>3.1</b>	<b>Contact time study</b>	<b>19</b>
<b>3.2</b>	<b>Adsorption rate order</b>	<b>22</b>
<b>3.3</b>	<b>Adsorption control mechanism</b>	<b>27</b>
<b>3.4</b>	<b>Conclusion</b>	<b>32</b>
	<b>References</b>	<b>33</b>

<b><u>Figures</u></b>		
<b><u>Fig. No.</u></b>	<b><u>Caption</u></b>	<b><u>Page No.</u></b>
<b>1</b>	Fig. 1 The contact time trend of CF sorption onto the ZnAl <sub>2</sub> O <sub>4</sub> nanocomposite	<b>20</b>
<b>2</b>	Fig. 2 The contact time trend of CF sorption onto the 2.5%NiO/ZnAl <sub>2</sub> O <sub>4</sub> composite.	<b>20</b>
<b>3</b>	Fig. 3 The contact time trend of CF sorption onto the 5%NiO/ZnAl <sub>2</sub> O <sub>4</sub> composite.	<b>21</b>
<b>4</b>	Fig. 4 The contact time trend of CF sorption onto the 10%NiO/ZnAl <sub>2</sub> O <sub>4</sub> composite.	<b>21</b>
<b>5</b>	Fig. 5 The PF investigation of CF sorption onto ZnAl <sub>2</sub> O <sub>4</sub> composite.	<b>23</b>
<b>6</b>	Fig. 6 The PF investigation of CF sorption onto 2.5%NiO/ZnAl <sub>2</sub> O <sub>4</sub> composite.	<b>23</b>
<b>7</b>	Fig. 7 The PF investigation of CF sorption onto 5%NiO/ZnAl <sub>2</sub> O <sub>4</sub> composite.	<b>25</b>
<b>8</b>	Fig. 8 The PS investigation of CF sorption onto ZnAl <sub>2</sub> O <sub>4</sub> composite.	<b>25</b>
<b>9</b>	Fig. 9 The PS investigation of CF sorption onto 2.5%NiO/ZnAl <sub>2</sub> O <sub>4</sub> composite.	<b>26</b>
<b>10</b>	Fig. 10 The PS investigation of CF sorption onto 5%NiO/ZnAl <sub>2</sub> O <sub>4</sub> composite.	<b>26</b>
<b>11</b>	Fig. 11 The LFD investigation of CF sorption onto ZnAl <sub>2</sub> O <sub>4</sub> composite.	<b>29</b>
<b>12</b>	Fig. 12 The LFD investigation of CF sorption onto 2.5%NiO/ZnAl <sub>2</sub> O <sub>4</sub> composite.	<b>29</b>
<b>13</b>	Fig. 13 The LFD investigation of CF sorption onto 5%NiO/ZnAl <sub>2</sub> O <sub>4</sub> composite.	<b>30</b>
<b>14</b>	Fig. 14 The IPD investigation of CF sorption onto ZnAl <sub>2</sub> O <sub>4</sub> composite.	<b>30</b>
<b>15</b>	Fig. 15 The IPD investigation of CF sorption onto 2.5%NiO/ZnAl <sub>2</sub> O <sub>4</sub> composite.	<b>31</b>
<b>16</b>	Fig. 16 The IPD investigation of CF sorption onto 5%NiO/ZnAl <sub>2</sub> O <sub>4</sub> composite.	<b>31</b>

## **Abstract**

This research used a rapid one-step method to synthesize MgSi-1, MgSi-2, MgSi-3, and MgSi-4. The resulting compounds were employed to remove ciprofloxacin CF from water by adsorption. The prepared MgSi-1, MgSi-2, MgSi-3, and MgSi-4 exhibited adsorption capacity  $q_t$  values of 72.4, 80.9, 89.1, and 97.8 mg/g, respectively, indicating that the introduction of MoO<sub>3</sub> onto MgOSiO<sub>2</sub> significantly enhanced the adsorption capacity of the matrix. It is worth noting that about 90% of the obtained  $q_t$  values were achieved within the first 20 to 30 min, and all adsorption processes reached equilibrium within 60 min, indicating that the produced compounds are candidates as adsorbents for rapid treatment of contaminated water. The adsorption order study showed that the CF removal process conformed to the pseudo-first-order adsorption rate, while the adsorption mechanism study showed that the CF removal by MgSi1, MgSi2, MgSi3 and MgSi4 was controlled by the diffusion step through the solution, which indicates that the four adsorbents have an excellent ability to remove the pharmaceutical pollutant CF through the adsorption process.

## الملخص باللغة العربية

في هذا البحث تم استخدام طريقة سريعاً من خطوة واحدة لتخليق مركبات  $\text{MgSi}$  و  $\text{MgSi-2}$  و  $\text{MgSi-1}$  من الماء عن طريق 3 و  $\text{MgSi-4}$  تم توظيف المركبات الناتجة لإزالة السيبروفلوكساسين CF من الماء عن طريق الامتزاز. أظهرت المركبات المحضرة  $\text{MgSi-1}$  و  $\text{MgSi-2}$  و  $\text{MgSi-3}$  و  $\text{MgSi-4}$  قيم سعة امتزاز 72.4 qt و 80.9 و 89.1 و 97.8 مجم / جم على التوالي، مما يشير إلى أن ادخال  $\text{MoO}_3$  على  $\text{MgOSiO}_2$  عزز من قدرة الامتزاز للمادة الأساسية بشكل ملحوظ. الجدير بالذكر ان حوالي 90% من قيم qt المتحصل عليها في تمت في غضون الـ 20 إلى 30 دقيقة الأولى، وبلغت جميع عمليات الامتزاز مرحلة الاتزان خلال 60 دقيقة، مما يشير إلى ترشيح المركبات المنتجة كمادة مازة للمعالجة السريعة للمياه الملوثة. اظهرت دراسة ترتيبية الامتزاز ان عملية ازالة CF وافقت معدل امتزاز الرتبة الاولى الكاذبة، بينما اظهرت دراسة ميكانيكية الامتزاز ان إزالة CF بواسطة  $\text{MgSi1}$  و  $\text{MgSi2}$  و  $\text{MgSi3}$  و  $\text{MgSi4}$  تحكمت فيها خطوة الانتشار عبر المحلول الامر الذي يدل على ان المواد المازة الاربعة لها قابلية ممتازة لازالة الملوث الصيدلاني CF عبر عملية الامتزاز.



# *Chapter One*

*Introduction  
and Literature Review*

## **1. Introduction**

### **1.1. Preparation of nanomaterials**

Numerous fields make use of nanoscale materials, including electronics, biology, medicine, cosmetics, ecology, materials science, magnetism, and environmental science [1]. The enormous potential of nanotechnology has prompted a worldwide upsurge in funding for related research and development. Both the amount of time and money spent on nanotechnology research has increased significantly since 1999. Greater social advancement and sustainable development are the primary goals of the researchers. If we can understand the steps involved in making nanoparticles, like those in combustion systems, we can come up with efficient ways to reduce the amount of pollutants and the amount of pollution they cause [2]. The bottom-up synthesis of nanomaterials involves combining atoms and molecules into molecules on the nanoscale. Methods for preparing nanomaterials include, and the second viewpoint is top-down, which involves reducing bulk materials to the nanoscale [3-5].

### **1.2. Common approaches for making nanomaterials**

#### **1.2.1. Sol-gel method**

The sol-gel process is a widely used nanomaterials technique. During a precursor reaction, a surfactant or nonaqueous solvent regulates the size of the particles in an appropriate solvent. The particles stopped small crystals from clumping together in a liquid medium. Numerous well-known chemists investigated the recurring precipitation processes that resulted in the creation of gel crystals and



Liesegang rings. [4, 6, 7]. This phenomena has prompted much descriptive investigation. Roy and his colleagues utilized the chemical homogeneity present in colloidal gels. They enhanced the sol-gel approach, enabling the synthesis of various ceramic oxide compositions incorporating Al, Si, Ti, Zr, etc., which were previously unattainable by ceramic powder techniques [8, 9]. The initial water and ammonia concentrations, precursor, solvent, and reactant temperatures dictate the ultimate size of the spherical particles [10, 11].

### **1.2.2. Solvothermal method**

The solvothermal (hydrothermal) technology, recognized for its environmental sustainability and potential, employs aqueous or nonaqueous solvents to enhance particle size distribution and shape regulation. This method standardizes metal salts and modifies the medium pH to alkaline using a basic solution. The target nanomaterial regulates the thermal treatment temperature and duration of the homogenized solution. Time, temperature, media, and precursors influence the dimensions and morphology of nanoparticles [12].

### **1.2.3. Green synthesis**

In the production of green nanomaterials, capping agents may consist of plant extracts or microorganisms. Plant-derived nanoparticles are created en masse for biosynthesis. Plants synthesize metallic nanoparticles from seeds, leaves, stems, roots, and latex. The most secure method for synthesizing nanoparticles was environmentally sustainable. The demand for the manufacture of green metallic nanoparticles has increased. We aim to eradicate synthetic waste, chemical

byproducts, and derivative substrates. Natural biomaterials are advantageous for the environmentally sustainable production of nanoparticles. Researchers utilize bacteria, algae, fungi, and plants to produce cost-effective, energy-efficient, and eco-friendly metal nanoparticles. Sustainable synthetic methods are supplanting physicochemical approaches in the sector [13, 14].

#### **1.2.4. Contamination of water**

Water is essential for human survival, as the deterioration of water quality impacts all forms of life. Organic contaminants in global water systems constitute a significant issue. Pharmaceuticals and chemical dyes are commonly utilized in water and sewage systems due to their extensive application and market demand. Water pollution is responsible for the majority of waterborne diseases, significantly impacting metropolitan populations. Consequently, individuals are compelled to consume untreated irrigation water, resulting in significant health repercussions [15].

Comprehending the origins, interactions, and consequences of water contaminants is crucial for mitigating their environmental impact and safeguarding ecosystems. The improper disposal of aging pollutants, decontamination equipment, and the elimination of substandard and contaminated human and animal waste products may introduce these pollutants into water systems [16-18]. Hazardous aquatic contamination renders the water supply systems of developed nations susceptible. The United States possesses more water than is produced by its rivers and lakes. Groundwater in certain

regions may be chemically dangerous. Water contaminants encompass heavy metals, chlorinated hydrocarbons, organic dyes, industrial metal coatings, and microbes. Since World War II, the manufacturing and utilization of synthetic chemicals have escalated. The existence of these pollutants has tainted water sources. Examples encompass pesticide use, agricultural effluent, and improper industrial waste dumping into aquatic bodies. Improper disposal of chemical waste in landfills, storage lagoons, treatment ponds, and other facilities can lead to groundwater contamination. Pollution and inequitable distribution restrict the accessibility of numerous global water sources, which seem boundless. Water scarcity impacts many individuals globally, triggering numerous conflicts. Groundwater, sourced by drilling, excavation, or springs, significantly impacts river baseflow. Approximately 80% of ocean pollutants originate from terrestrial sources, either industrial activities or indirect disposal of human waste [19-21]. The Netherlands conducted nationwide surveillance from 2010 to 2014. The operation identified elevated pesticide concentrations in groundwater wells, which is concerning. This research analyzed shallow groundwater samples from the Netherlands and Flanders for 405 chemicals and 52 metabolites. The findings indicated the presence of neonicotinoids, which are both mobile and persistent, at concentrations ranging from 0.12 to 0.01 g/L [22]. The Yangtze River Basin in Hubei Province, Central China, exhibited elevated levels of organochlorine and organophosphate pesticides. Sixteen groundwater samples from the specified area contained fifteen organochlorine compounds and four

organophosphate compounds. The mean concentrations of the four organophosphate pesticides were 196.01 ng/L for aldrin, dieldrin, and hexachlorocyclohexane. The water supply failed to comply with EPA standards [23]. The phreatic aquifer underlying the Pampean region of Argentina harbors organochlorine pesticides, signifying their prolonged presence. Numerous studies indicate that specific regions exhibit elevated levels of fluoride in groundwater. Refrain from utilizing groundwater with elevated fluoride levels for extended periods. The health advantages of fluoride warrant the fluoridation of public water supplies. Excessive fluoride absorption can lead to dental and skeletal fluorosis. This study found that neonates and toddlers exhibit heightened sensitivity to dental fluorosis, a non-carcinogenic danger. A recent investigation of groundwater fluoride levels in Agra City, India, revealed a significant variation above the WHO guideline of 1.5 mg/L. The mean fluoride concentration in 51 groundwater samples from Siddipet Vagu, India, was 3.7 ppm. 51% of samples surpassed the WHO safety threshold of 1.5 mg/L for fluoride [24]. The research analyzed fifty borehole samples from dense agricultural regions along the West Bank of the Nile River in Luxor Governorate, Egypt, revealing that 62% exhibited moderate vulnerability to groundwater contamination, while 38% demonstrated high vulnerability. Nitrate contamination from nitrogen-based fertilizers has affected 52% of the land. Recent research indicated that Chungcheong Province, South Korea, exhibited a mean nitrate concentration of 12.4 mg/L [25]. Pharmaceutical pollutants

(PhCs) are present in groundwater, oceans, and rivers globally. Articulating the grave predicament of humanity may prove beneficial: Since 1970, 50% of Earth's water has been contaminated. In 1999, the United States recognized PhC-contaminated water as a public health hazard [26-29]. More than fifty percent of China's population consumed contaminated water during that period. Indian rivers, groundwater, and water treatment facilities harbor pharmaceutical contaminants. These compounds may attain concentrations of  $31.0 \text{ mg L}^{-1}$  [30, 31]. The demand for infectious illness therapies and the increasing production of agriculture, poultry, and livestock contribute to PhC pollution. Among these drugs ciprofloxacin (CF) was widely used in the last two decades. Numerous investigations have identified TCs in soil and water reservoirs in the United States, United Kingdom, and China [32]. The proliferation of pharmaceutical contaminants in marine, freshwater, and potable water sources indicates the inadequacy of existing treatment methodologies [33-41]. Consequently, PhC prevention necessitates innovative approaches. Nanomaterials have enhanced the adsorption process, effectively eliminating non-degradable water pollutants such as heavy metals. This technique is straightforward, energy-efficient, and does not emit detrimental byproducts.

### **1.3. Aim of the study**

This study aimed to prepare  $\text{MgO/SiO}_2$  (MgSi-1),  $2.5\% \text{MoO}_3 @ \text{MgO/SiO}_2$  (MgSi-2),  $5\% \text{MoO}_3 @ \text{MgO/SiO}_2$  (MgSi-3), and  $10\% \text{MoO}_3 @ \text{MgO/SiO}_2$  (MgSi-4) triple composite as environmentally safe sorbents. A one-put route was

adopted in order to simplify the process. The prepared double and triple composites will be tested for removing organic pollutants exemplified by CF, and their sorption kinetics will be investigated.



# *Chapter Two*

## *Materials and Methods*

## **2. Materials and methods**

### **2.1 Materials**

CF was provided from Rhanboxy, Mumbai, india. magnesium oxide (MgO) was provided from Fluka, USA. Molebdtinum oxide ( $\text{MoO}_3$ ) and D(+)-Glucose monohydrate (GL) were provided from Riedel-de-Haen, Germany. Fumed silica ( $\text{SiO}_2$ ) was purchased from (LOBA CHEMIE, Mumbai, India).

### **2.2. Preparation of MgSi- nanocomposites**

Equal moles of MgO and  $\text{SiO}_2$ , were were transferred to a 500 mL beaker. 10 g of GL and 50 mL of distilled water were added to the beaker. The mixture was heated on a hotplate until the GL was carbonized. The obtained powder was grinded, transferred to a porcelain dish, and calcined at  $600^\circ\text{C}$  for 3.0 h. The process was repeated using the typical MgO and  $\text{SiO}_2$  amounts with the addition of a proper amount of  $\text{MoO}_3$  to obtain MgSi-2, MgSi-3, and MgSi-4 triple composites.

### **2.3. Preparation of CF solution**

0.1g of CF was weighed using an analytical balance and transferred to a 1L volumetric flask to obtain  $100 \text{ mg L}^{-1}$  CF solution. Then, 600 mL of DW was added to the flask and put into an ultrasonic path, then the solution was completed with DW to the neck mark.

### **2.4. CF Adsorption**

0.05g of sorbent was weighed in 150 mL beaker. 100 mL of the  $100 \text{ mg L}^{-1}$  CF solution was poured into the beaker. A portion of the mixture was withdrawn till



the CF sorption reached the equilibrium. The aliquots were filtered via a 0.22 $\mu$ m syringe filter, and the absorbance was measured utilizing a UV-Vis-spectrophotometer ( $\lambda_{\text{max}} = 273 \text{ nm}$ ).



# *Chapter Three*

*Results and discussion*

### 3.1. Contact time study

The contact time study of CF and sorption onto the as-prepared nanocomposite was studied. The CF and absorbance measured during the study were employed for calculating their remaining concentrations (unadsorbed) at each time interval via Eq. 1. Using Eq. 2 was utilized to calculate the adsorption capacity at each period (the CF or milligrams adsorbed onto one gram of sorbent,  $q_t$ ,  $\text{mg g}^{-1}$ ).

$$C_t = \frac{\text{Absorbance}_{\text{sample}}}{\text{Absorbance}_{\text{standard}}} \times \text{conc.}_{\text{standard}} \quad (1)$$

$$q_t = \frac{(C_o - C_t) V}{m}, \quad (2)$$

Fig. 1 demonstrate the adsorption trend of CF onto prepared nanocomposite. The MgSi-1, MgSi-2, MgSi-3, and MgSi-4 triple composites showed  $q_t$  values of 72.4, 80.9, 89.1, and 97.8  $\text{mg/g}$ . Although all sorption processes reached equilibrium within 90 minutes, almost 90% of the gained  $q_t$  values was acquired within the first 30 minutes, reflected high sorption ability of the MgSi to treat contaminated water and nominating them as fast treatment sorbents.

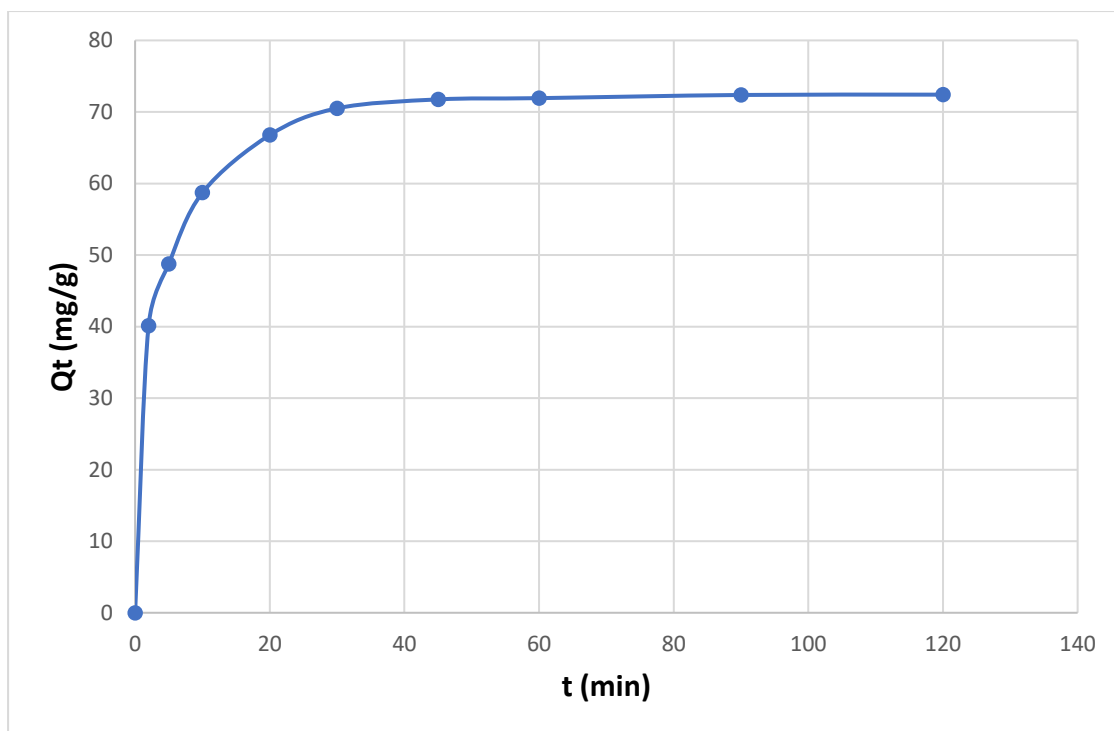


**Fig. 1** The contact time results of CF sorption onto MgSi-1 composite.

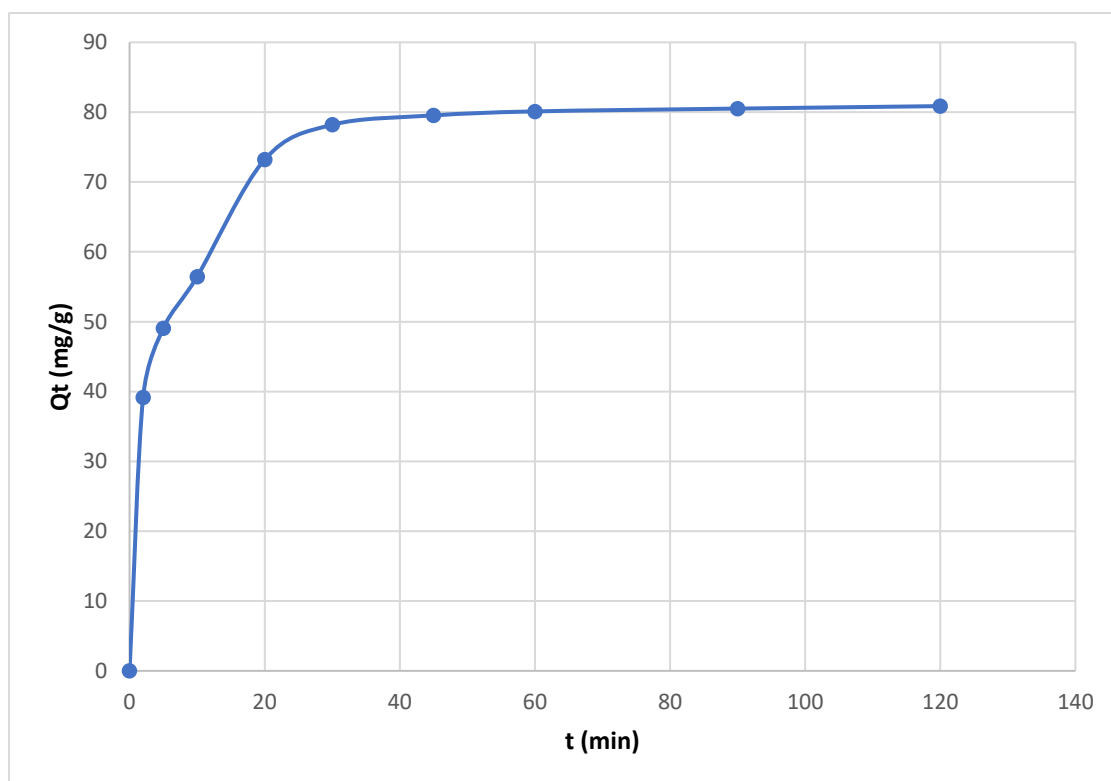


**Fig. 2** The contact time results of CF sorption onto MgSi-2 composite.

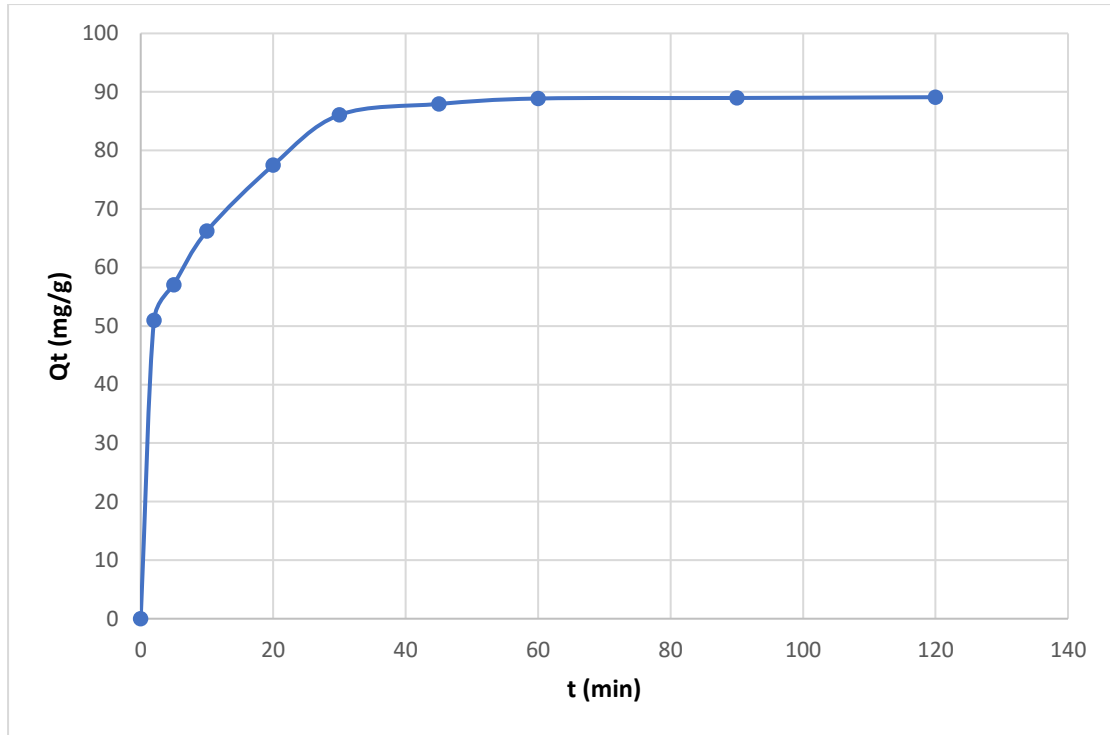


**Fig. 3** The contact time results of CF sorption onto MgSi-3 composite.

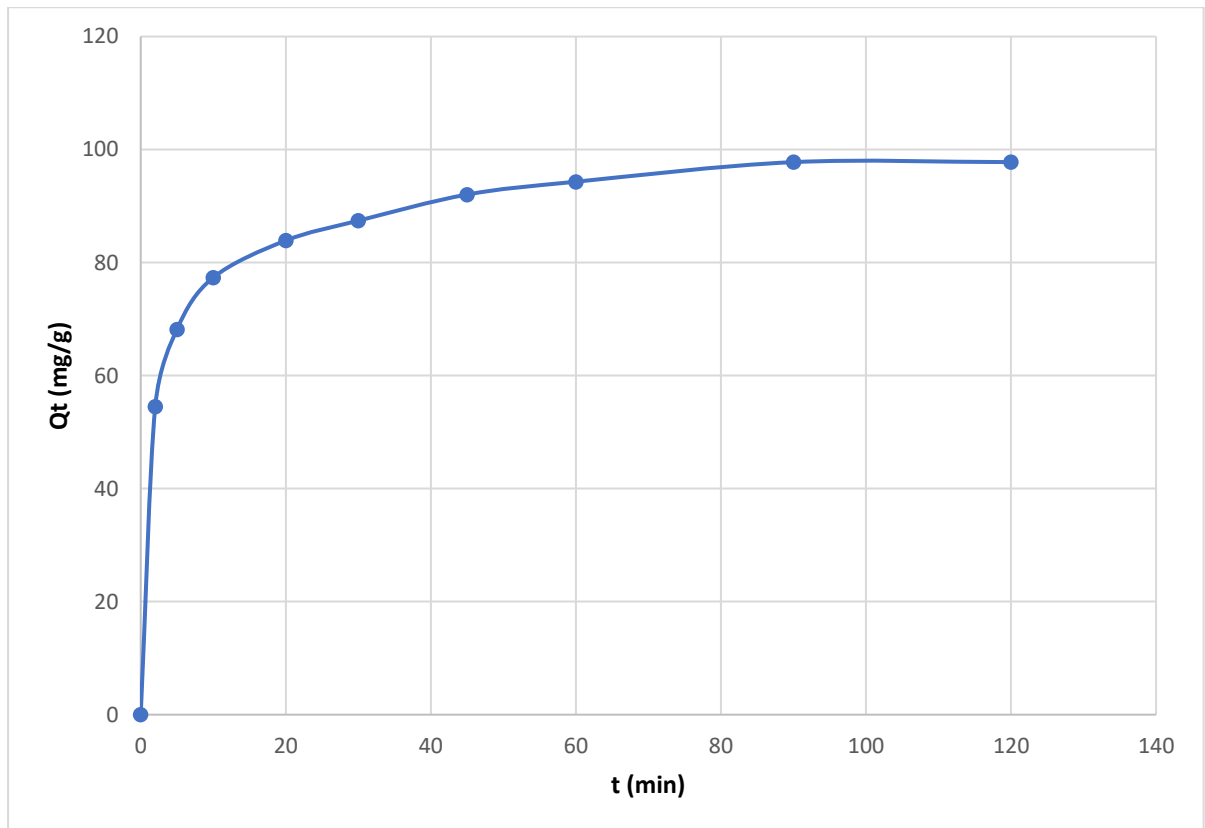


**Fig. 4** The contact time results of CF sorption onto MgSi-4 composite.

### 3.2 Adsorption rate order

The adsorption rate order of CF and removal by was studied via pseudo-first-order (PF, Eq. 3) and pseudo-second-order (PS, Eq. 4) kinetic models.

$$\ln(q_e - q_t) = \ln q_e - k_1 \cdot t \quad (3)$$

$$\frac{1}{q_t} = \frac{1}{k_2 \cdot q_e^2 t} + \frac{1}{q_e} \quad (4)$$

The symbol  $q_e$  (mg g<sup>-1</sup>) represents the equilibrium adsorption capacity. The PF and PS constants are also time-dependent, with the former represented as  $k_1$  (min<sup>-1</sup>) and the latter as  $k_2$  (g mg<sup>-1</sup> min<sup>-1</sup>). The PF plots of the CF adsorption onto MgSi-1, MgSi-2, MgSi-3, and MgSi-4 composite were depicted in Fig. 5, 6, 7, and 8, respectively, while the PS plots were illustrated in Fig. 9, 10, 11, and 12, respectively. The rate-order output of CF removal by the four composites showed better fitting to the PF model (Table 1).

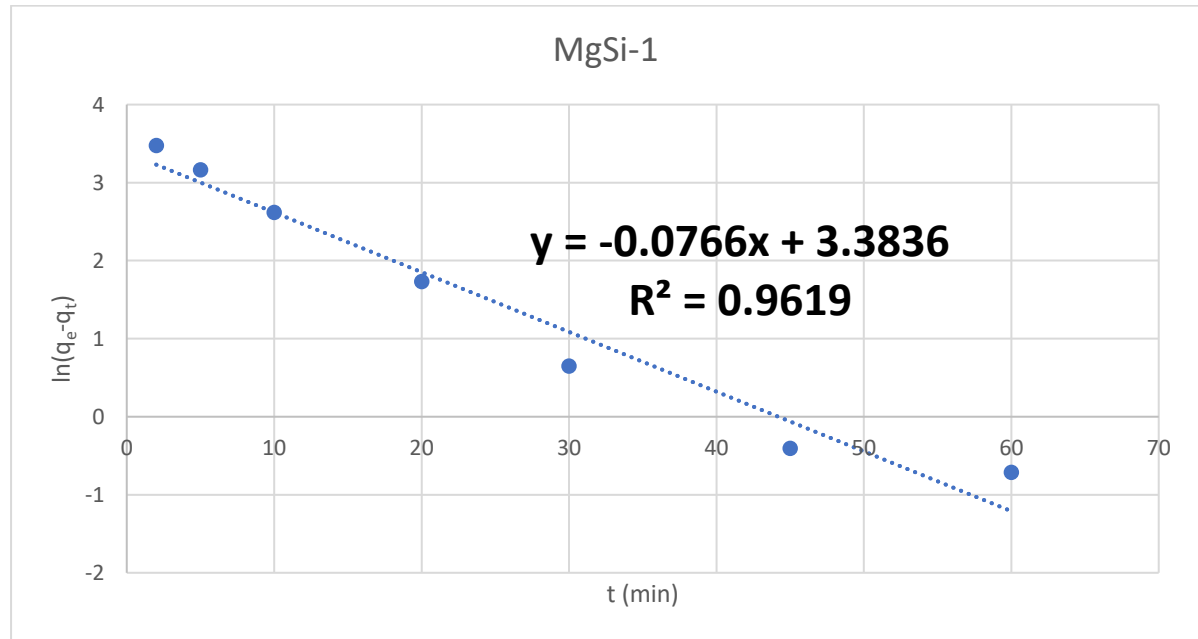


**Fig. 5** The PF investigation of CF sorption onto MgSi-1 composite.

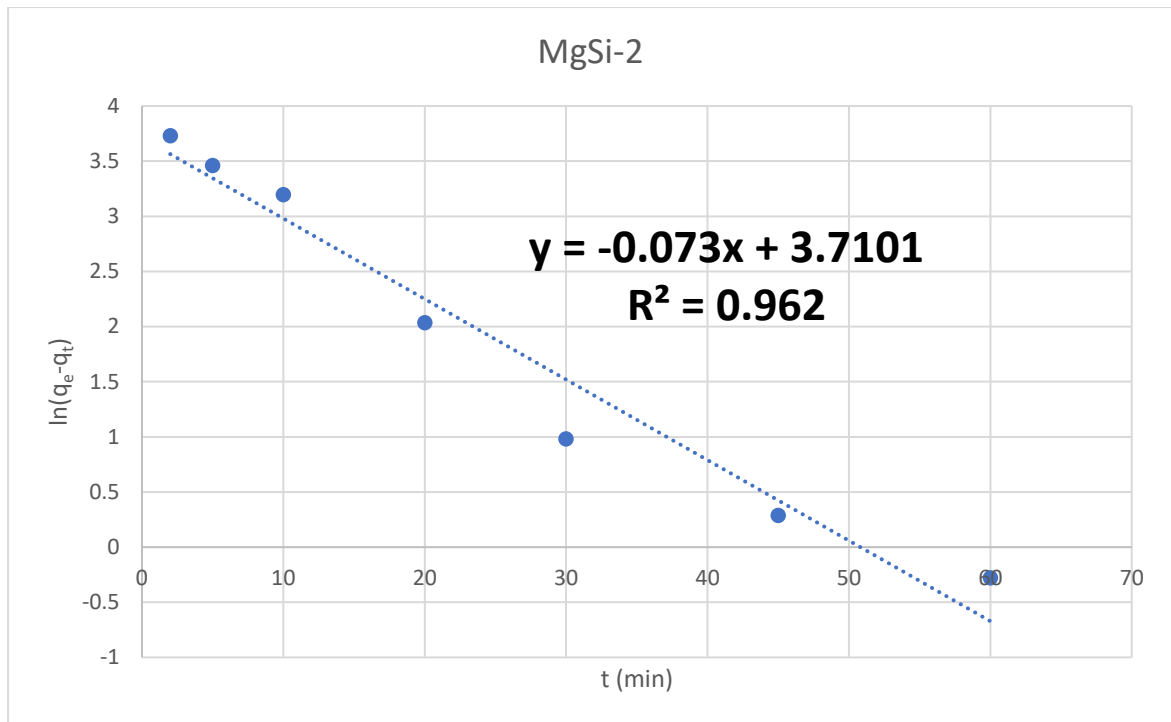


**Fig. 6** The PF investigation of CF sorption onto MgSi-2 composite.

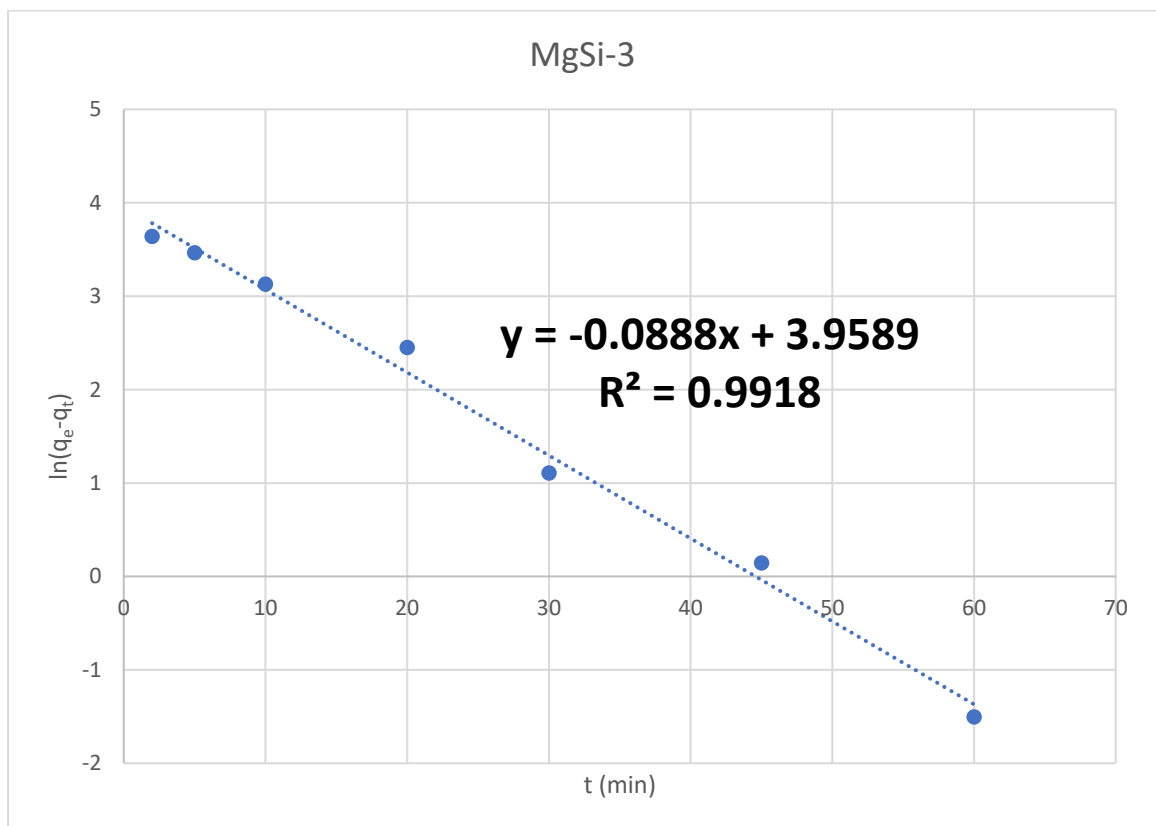


**Fig. 7** The PF investigation of CF sorption onto MgSi-3 composite.

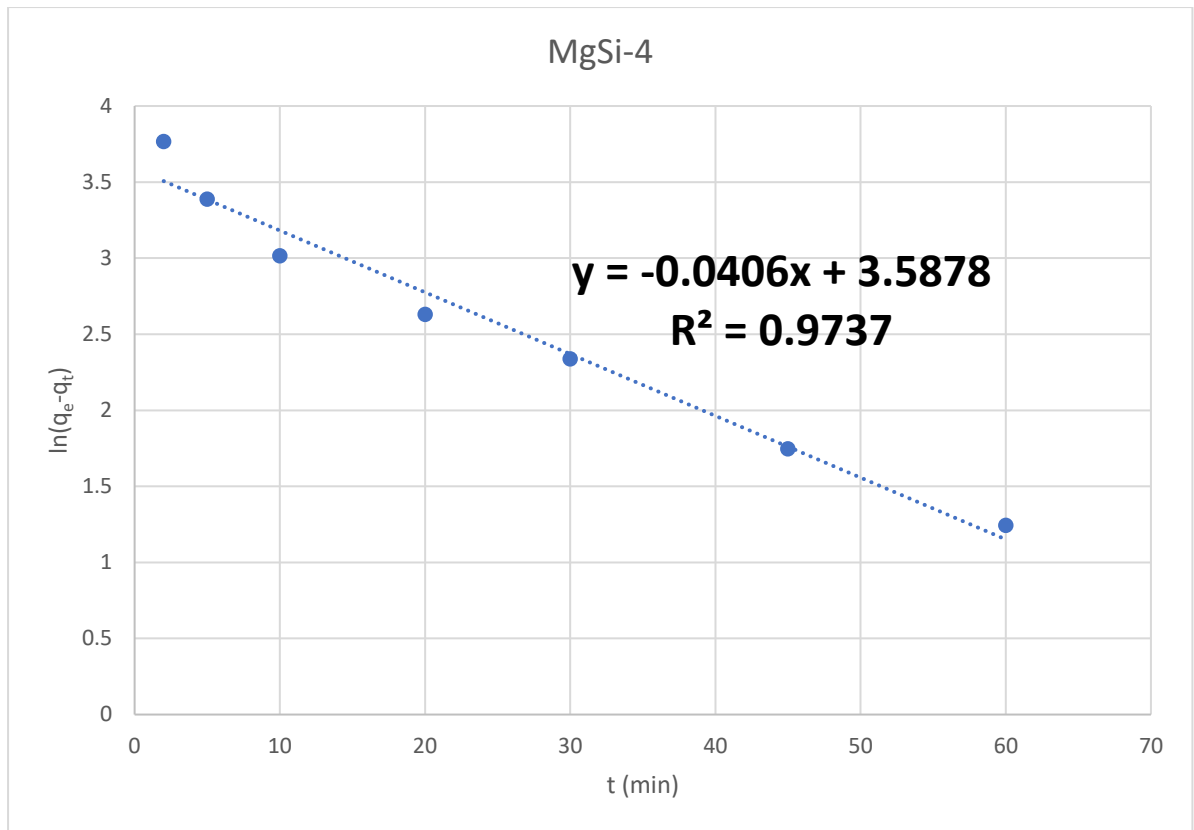


**Fig. 8** The PF investigation of CF sorption onto MgSi-4 composite.

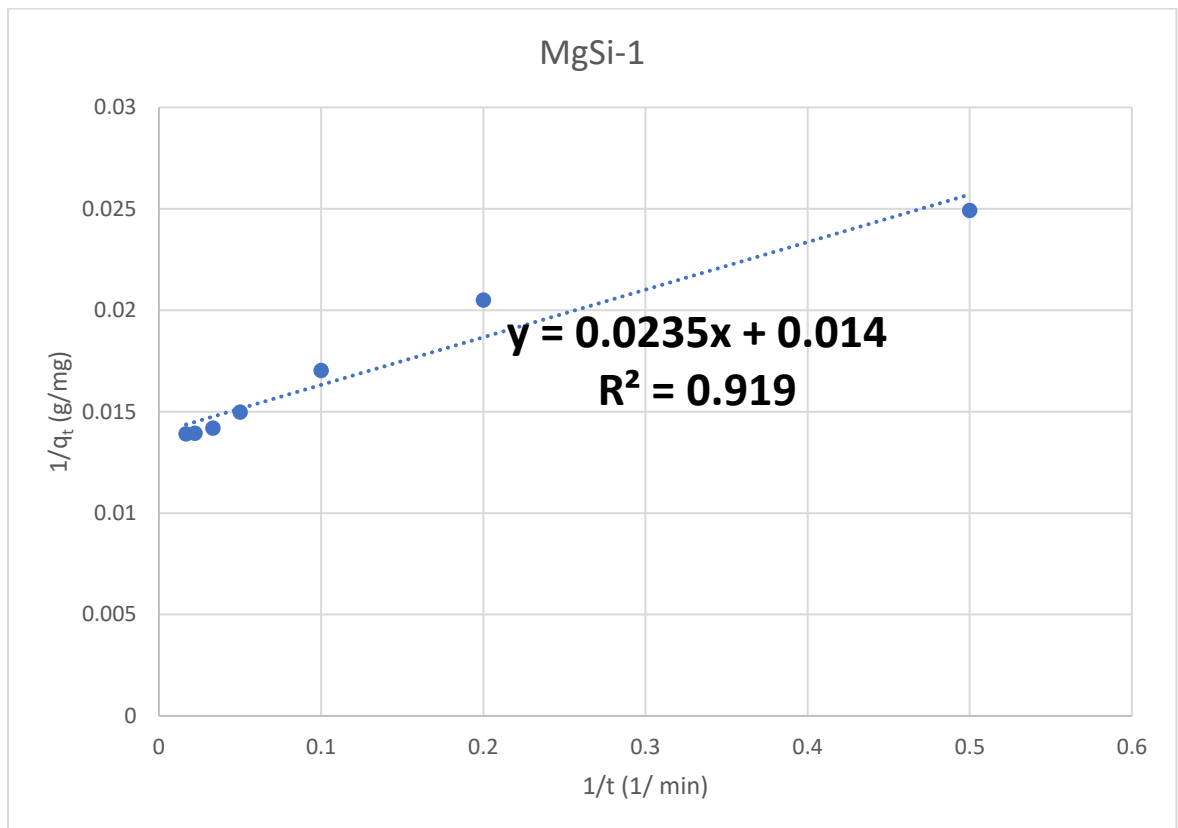


**Fig. 9** The PS investigation of CF sorption onto MgSi-1 composite.



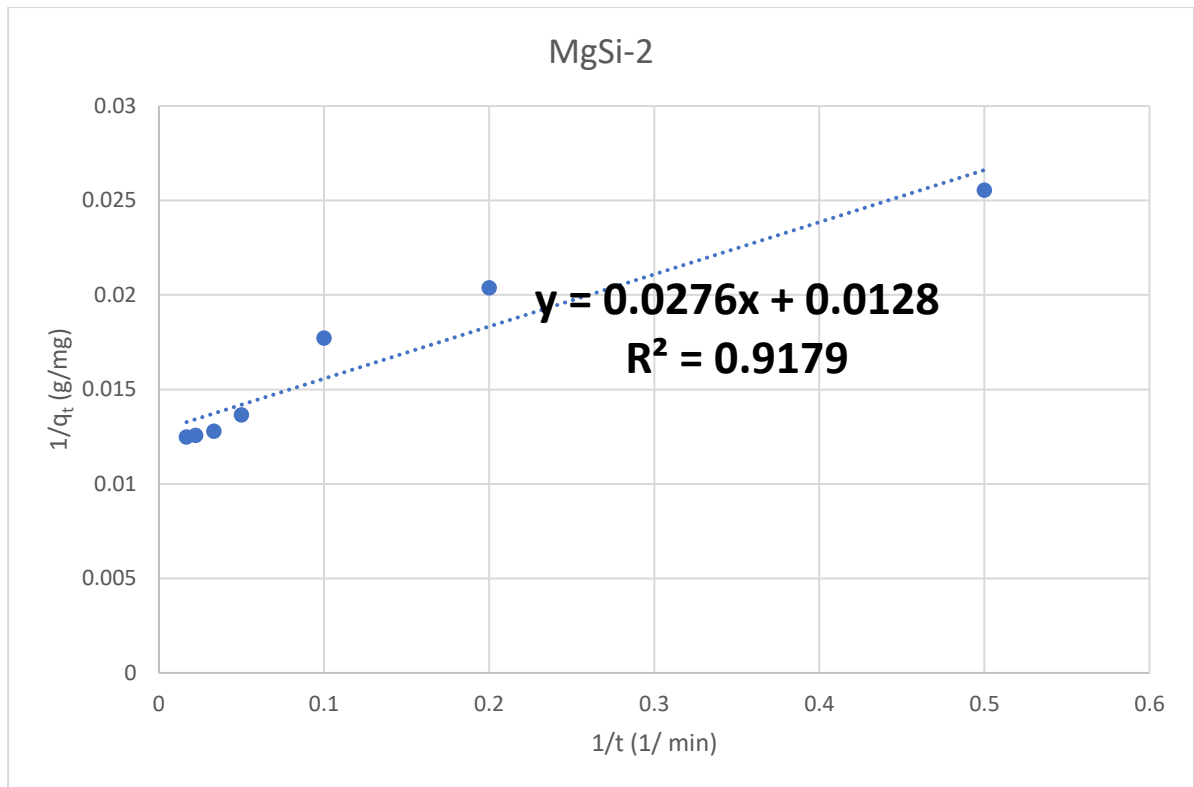


**Fig. 10** The PS investigation of CF sorption onto MgSi-2 composite.

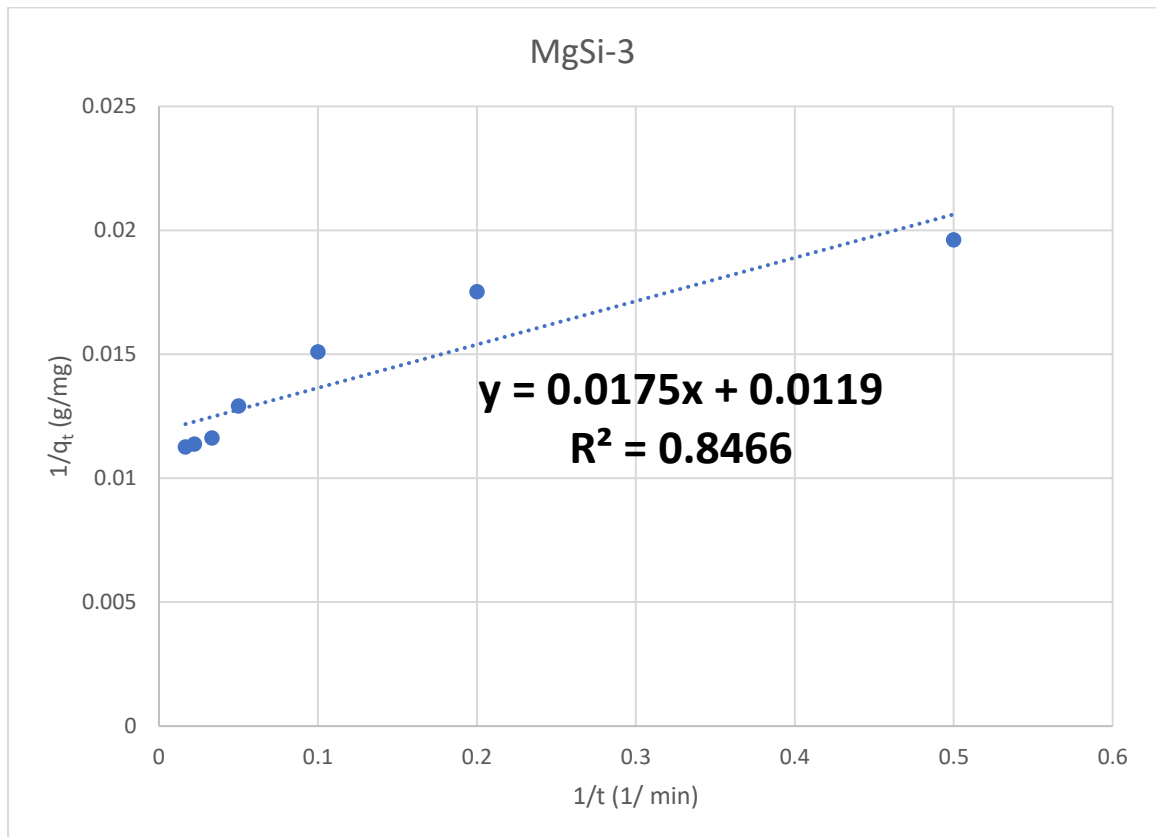


**Fig. 11** The PS investigation of CF sorption onto MgSi-3 composite.

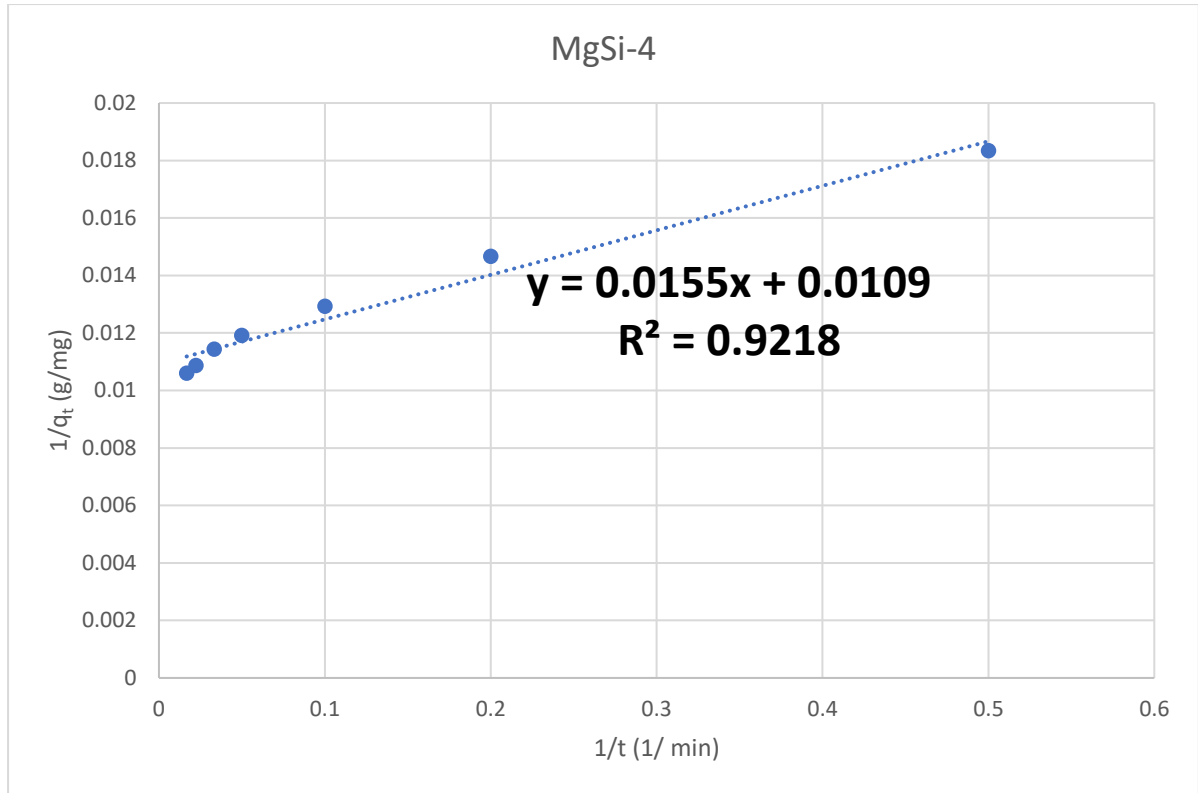


**Fig. 12** The PS investigation of CF sorption onto MgSi-4 composite.

**Table 1** The adsorption rate order results of CF removal by MgSi-1, MgSi-2, MgSi-3, and MgSi-4 composites.

Adsorbent	qe exp. (mg g <sup>-1</sup> )	PFO		PSO	
		R2	k1	R2	k2
MgSi-1	72.43	0.962	0.077	0.919	0.008
MgSi-2	80.87	0.962	0.073	0.918	0.006
MgSi-3	89.10	0.992	0.089	0.847	0.008
MgSi-4	97.78	0.974	0.041	0.922	0.008

### 3.3 Adsorption control mechanism

The rate-control mechanism of CF and removal by MgSi-1, MgSi-2, MgSi-3, and MgSi-4 composites was studied using the intraparticle (IPD, Eq. 5) and the liquid-film (LFD, Eq. 6) diffusion model.

$$q_t = K_{IP} * t^{\frac{1}{2}} + C_i \quad (5)$$

$$\ln(1 - F) = -K_{LFD} * t \quad (6)$$

The IPD constant is denoted by  $K_{IPD}$  ( $\text{mg g}^{-1} \text{min}^{-1/2}$ ), and the LFD constant is designated by  $K_{LFD}$  ( $\text{min}^{-1}$ ).  $C_i$ : the boundary layer factor, expressed as  $\text{mg g}^{-1}$ .

The LFD plot of the CF adsorption onto MgSi-1, MgSi-2, MgSi-3, and MgSi-4 composite were depicted in Fig. 13, 14, 15, and 16, respectively, while the IPD plots were illustrated in Fig. 17, 18, 19, and 20, respectively. The rate-control output of CF removal by the four composites fitted the LFD indicating high sorbent-sorbate affinity (Table 2).

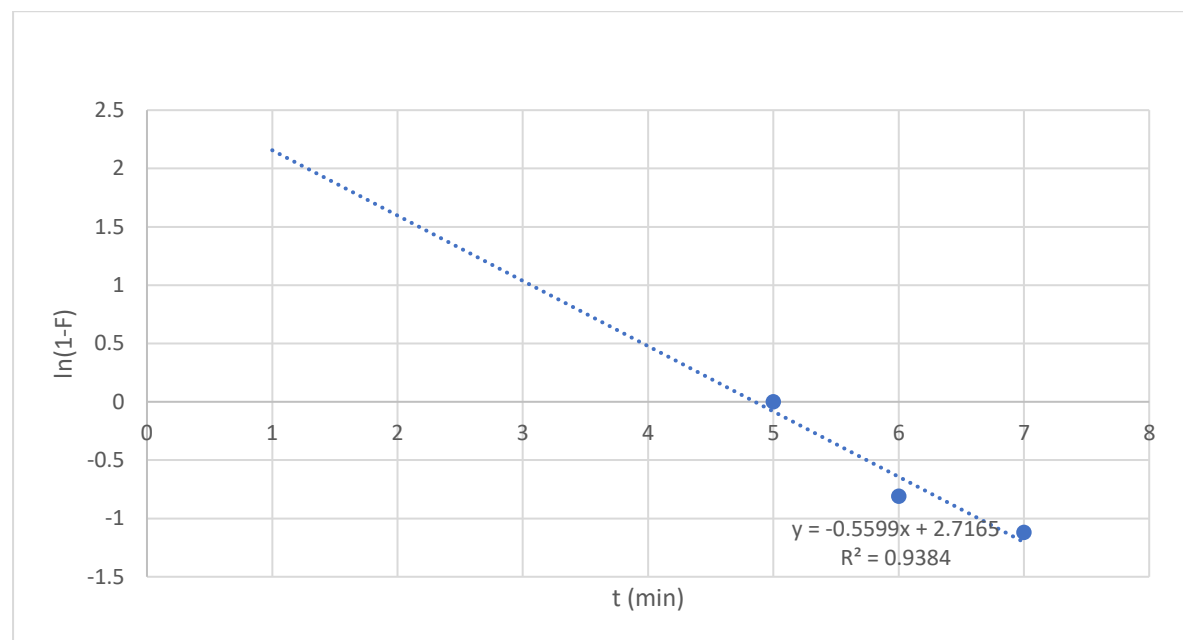


**Fig. 13 The LFD study of CF sorption onto MgSi-1 composite.**

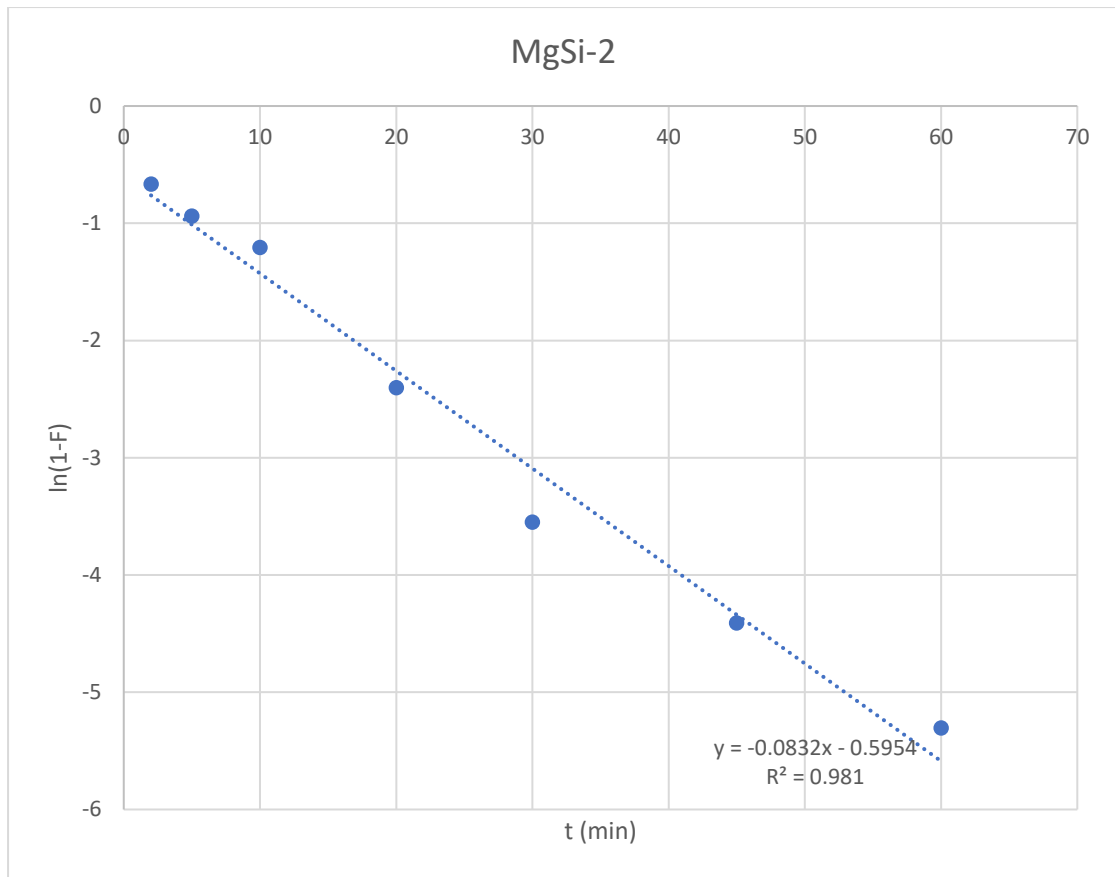


**Fig. 14 The LFD study of CF sorption onto MgSi-2 composite.**

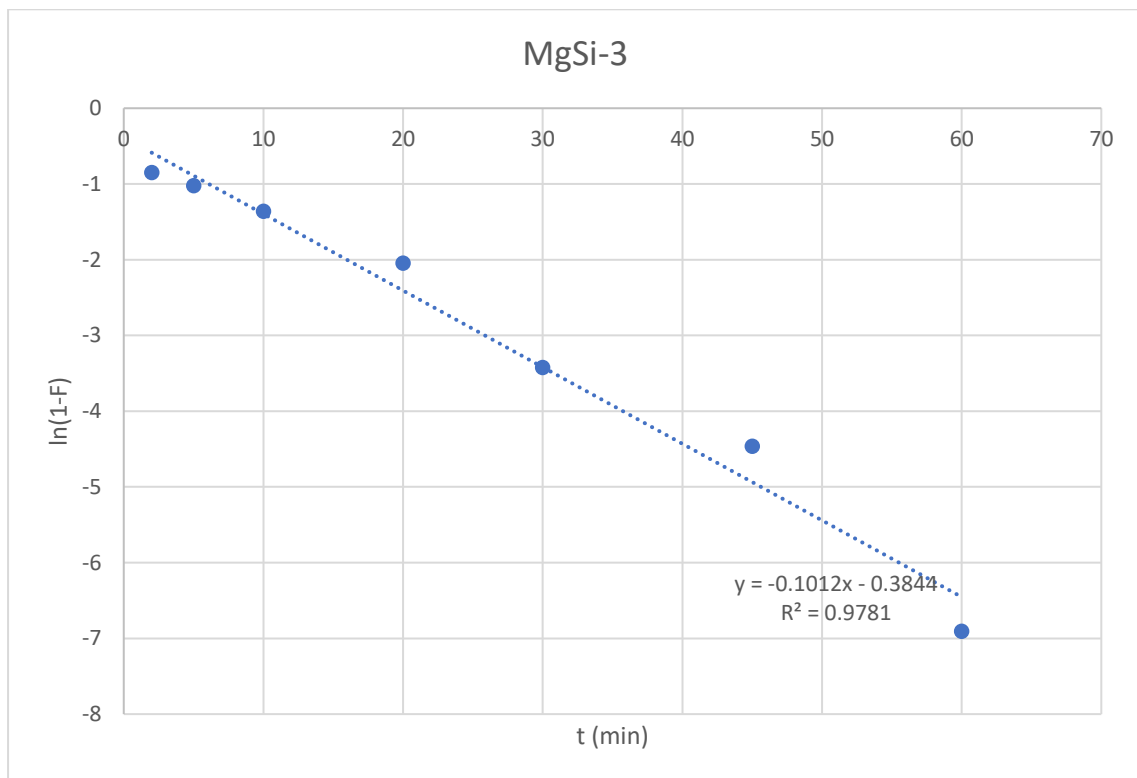


**Fig. 15 The LFD study of CF sorption onto MgSi-3 composite.**

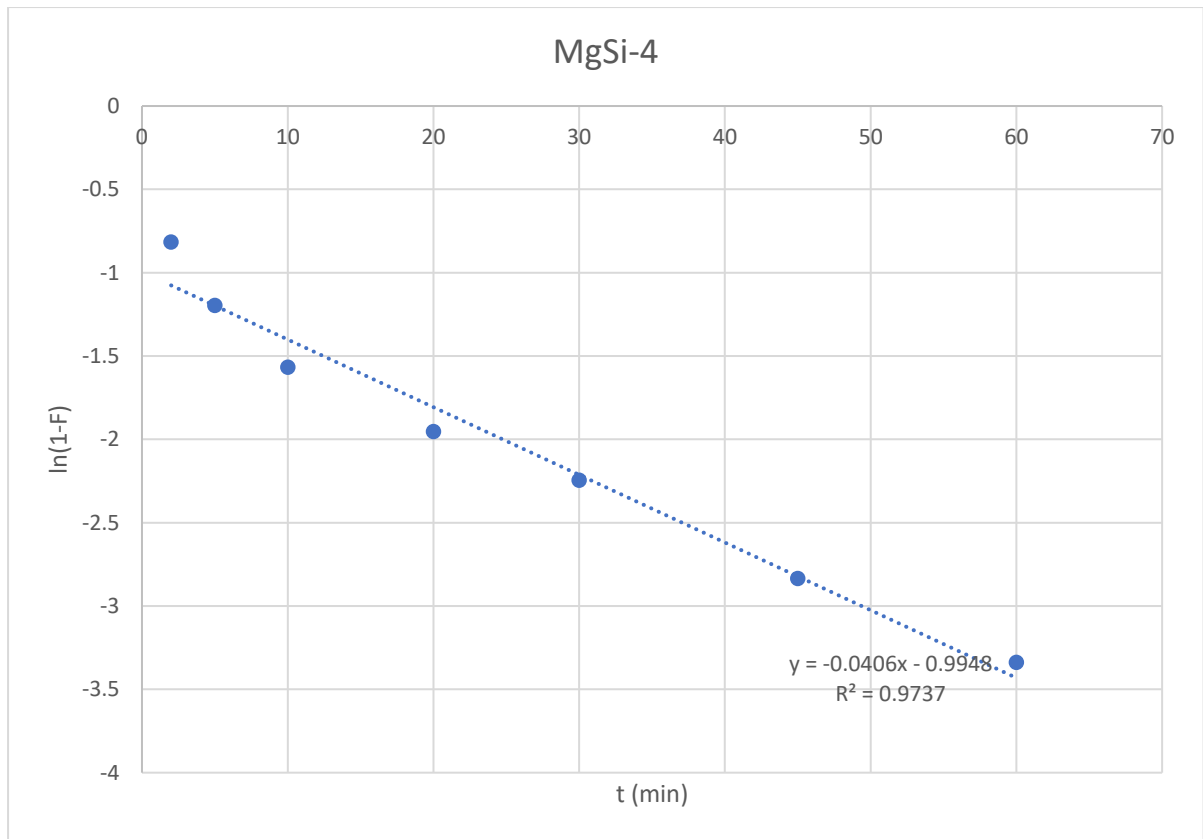


**Fig. 16 The LFD study of CF sorption onto MgSi-4 composite.**

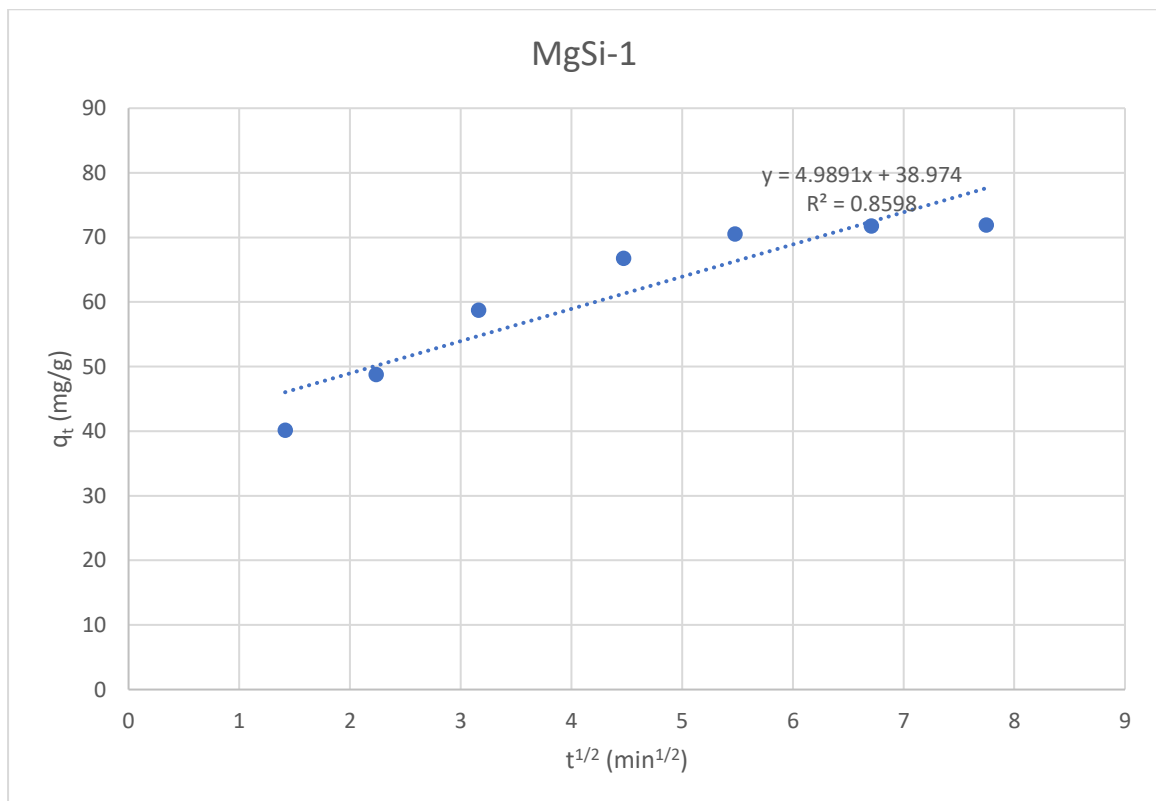


**Fig. 17 The IPD study of CF sorption onto MgSi-1 composite.**

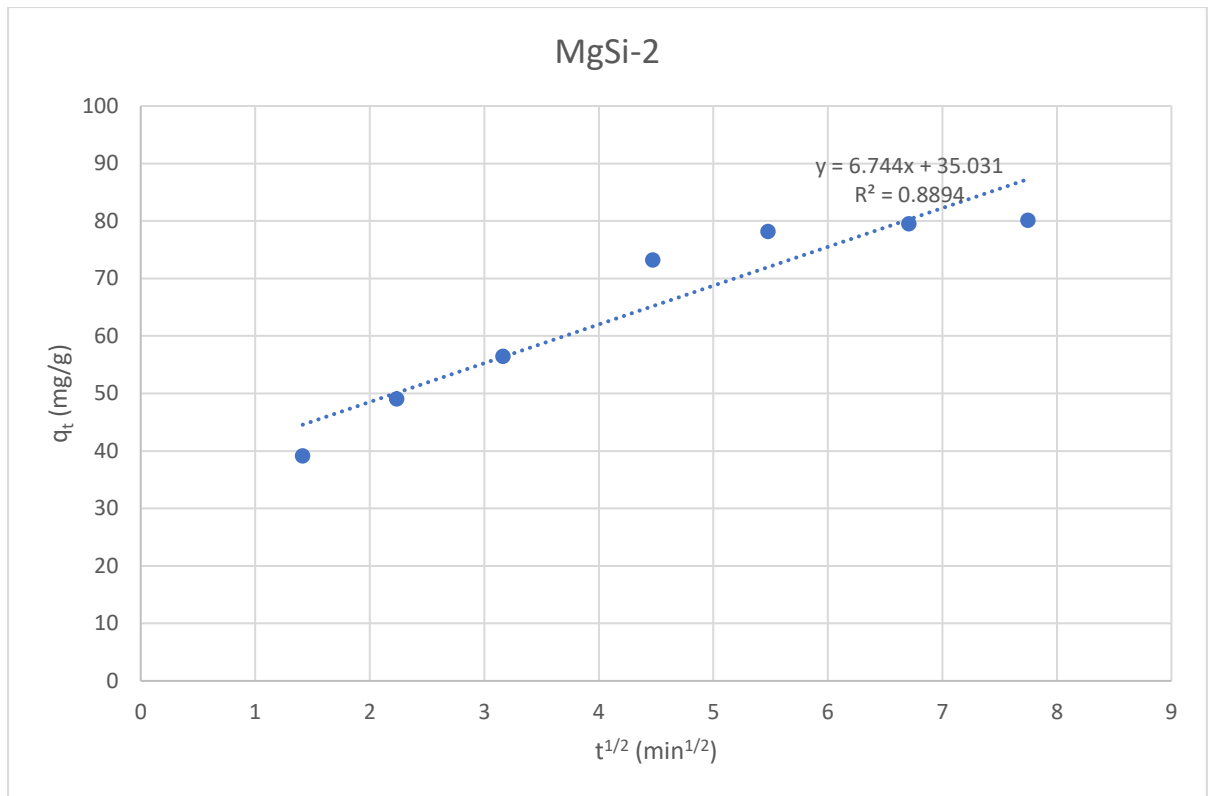


**Fig. 18** The IPD study of CF sorption onto MgSi-2 composite.

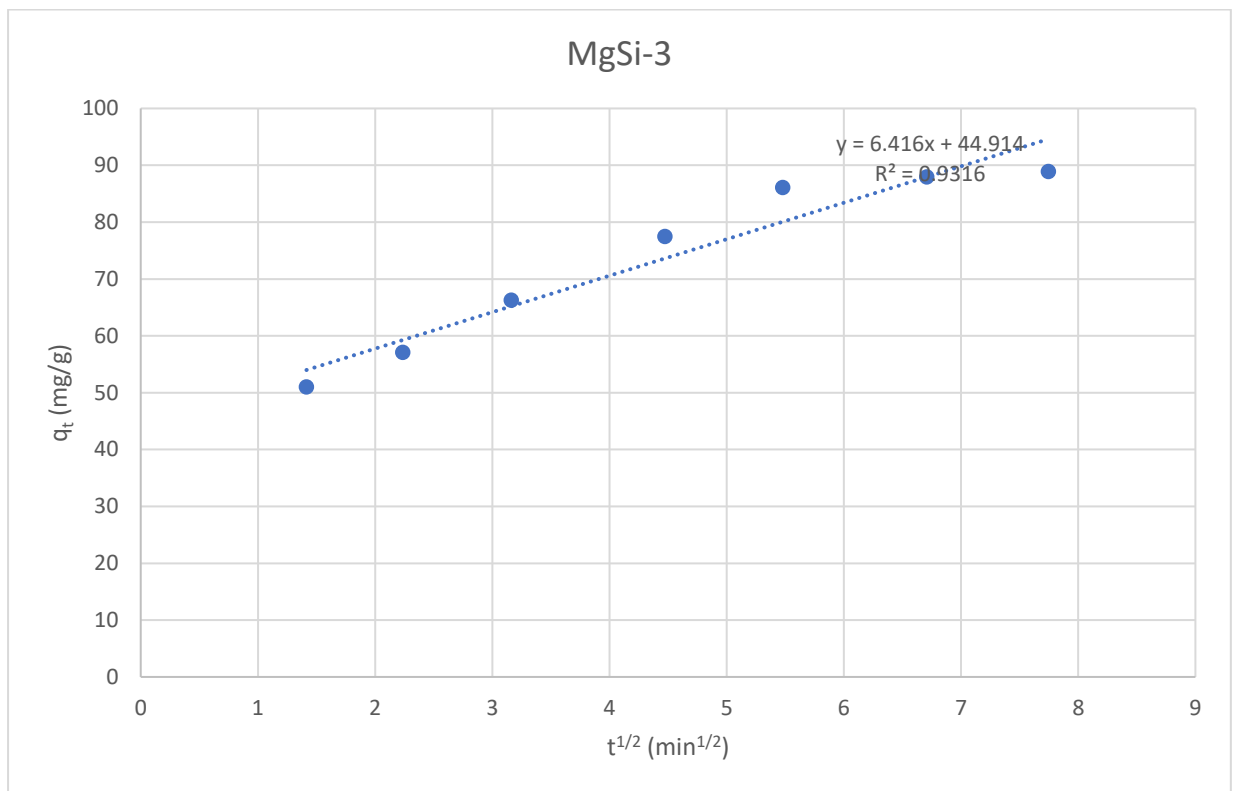


**Fig. 19** The IPD study of CF sorption onto MgSi-3 composite.

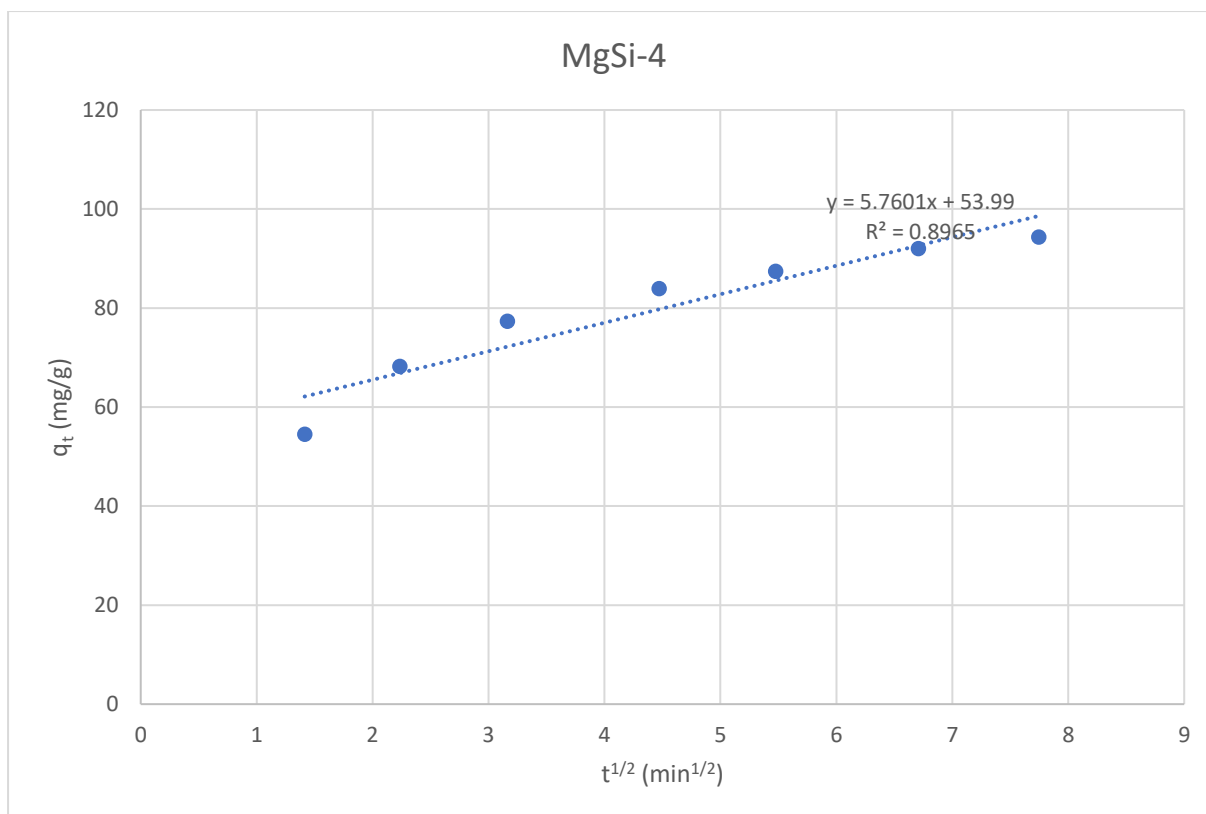


**Fig. 20** The IPD study of CF sorption onto MgSi-4 composite.

**Table 1** The adsorption rate control results of CF removal by MgSi-1, MgSi-2, MgSi-3, and MgSi-4.

Adsorbent	LFDM		IPDM	
	$K_{LF}$ (min <sup>-1</sup> )	$R^2$	$K_{IP}$ (mg g <sup>-1</sup> min <sup>0.5</sup> )	$R^2$
MgSi-1	0.078	0.965	4.989	0.859
MgSi-2	0.083	0.981	6.744	0.889
MgSi-3	0.101	0.978	6.416	0.931
MgSi-4	0.041	0.974	5.760	0.896

### 3.4. Conclusion

This study used a one-put fast method to prepare MgSi-1, MgSi-2, MgSi-3, and MgSi-4 composites. The synthesized composites were studied for removing CF and from the water via adsorption. The MgSi-1, MgSi-2, MgSi-3, and MgSi-4 showed  $q_t$  values of 72.4, 80.9, 89.1, and 97.8 mg/g, respectively, these results reflected that doping MgOSiO<sub>2</sub> with MoO<sub>3</sub> improved the sorption ability of the base material. Notably, almost 90% of the gained  $q_t$  values were acquired within the first 20 to 30 minutes, and all sorption processes reached equilibrium at 60 minutes, which nominated the prepared composites as fast treatment sorbents. The rate-order output of CF removal by MgSi-1, MgSi-2, MgSi-3, and MgSi-4 followed the PF model, and the rate-control output revealed that that the LF controlled the CF sorption onto the four sorbents.



## References

1. Hasan, S.J.R.J.R.S., *A review on nanoparticles: their synthesis and types*. 2015. **2277**: p. 2502.
2. Biswas, P., C.-Y.J.J.o.t.a. Wu, and w.m. association, *Nanoparticles and the environment*. 2005. **55**(6): p. 708-746.
3. Tissue, B. and H.J.J.o.S.S.C. Yuan, *Structure, particle size, and annealing of gas phase-condensed Eu<sup>3+</sup>: Y<sub>2</sub>O<sub>3</sub> nanophosphors*. 2003. **171**(1-2): p. 12-18.
4. Hasany, S., et al., *Systematic review of the preparation techniques of iron oxide magnetic nanoparticles*. 2012. **2**(6): p. 148-158.
5. Arole, V. and S.J.J.M.S. Munde, *Fabrication of nanomaterials by top-down and bottom-up approaches-an overview*. 2014. **1**: p. 89-93.
6. Minemoto, T., et al., *Preparation of Zn<sub>1-x</sub>Mg<sub>x</sub>O films by radio frequency magnetron sputtering*. 2000. **372**(1-2): p. 173-176.
7. Ostwald, W.J.P.C., *On the Formation of Liesegang Rings*. 1897. **27**: p. 365.
8. Rayleigh, L.J.T.L., Edinburgh,, D.P. Magazine, and J.o. Science, *LXXVIII. Periodic precipitates*. 1919. **38**(228): p. 738-740.
9. Alexander, J., *Colloid Chemistry, Theoretical and Applied: Theory and methods*. Vol. 1. 1926: Chemical Catalog Company.
10. Stöber, W., et al., *Controlled growth of monodisperse silica spheres in the micron size range*. 1968. **26**(1): p. 62-69.
11. Tan, C., et al., *Production of monodisperse colloidal silica spheres: Effect of temperature*. 1987. **118**(1): p. 290-293.
12. Houshiar, M., et al., *Synthesis of cobalt ferrite (CoFe<sub>2</sub>O<sub>4</sub>) nanoparticles using combustion, coprecipitation, and precipitation methods: A comparison study of size, structural, and magnetic properties*. 2014. **371**: p. 43-48.
13. Tadic, M., et al., *Magnetic properties of novel superparamagnetic iron oxide nanoclusters and their peculiarity under annealing treatment*. 2014. **322**: p. 255-264.
14. Sun, C., et al., *Versatile application of a modern scanning electron microscope for materials characterization*. 2020. **55**(28): p. 13824-13835.
15. Manahan, S., *Environmental chemistry*. 2017: CRC press.
16. Ruhoy, I.S. and C.G.J.E.i. Daughton, *Beyond the medicine cabinet: an analysis of where and why medications accumulate*. 2008. **34**(8): p. 1157-1169.
17. Zhao, Y. and X. Xiao, *Environmental Antibiotics: Exposure Monitoring and Health Endpoints*, in *Emerging Chemicals and Human Health*. 2019, Springer. p. 165-178.
18. Gupta, R., B. Sati, and A. Gupta, *Treatment and recycling of wastewater from pharmaceutical industry*, in *Advances in Biological Treatment of Industrial Waste Water and their Recycling for a Sustainable Future*. 2019, Springer. p. 267-302.
19. MISHRA, R., et al., *INVESTIGATION OVER WATER QUALITY OF RIVERS GANGA AND YAMUNA DURING KUMBH-2019-A CASE STUDY AT PRAYAGRAJ (ALLAHABAD), UTTAR PRADESH, INDIA*.
20. Yihdego, Z.J.B.R.P.i.I.W.L., *The fairness 'dilemma' in sharing the Nile waters: what lessons from the grand Ethiopian renaissance dam for international law?* 2017. **2**(2): p. 1-80.
21. Verma, J., et al., *Marine pollution, sources, effect and management*. Three Major Dimensions of Life: Environment, Agriculture and Health. Prayagraj, India: Society of Biological Sciences and Rural Development, 2020: p. 270-276.
22. Sjerps, R.M., et al., *Occurrence of pesticides in Dutch drinking water sources*. 2019. **235**: p. 510-518.
23. Pan, Z., et al., *Environmental implications of microplastic pollution in the Northwestern Pacific Ocean*. 2019. **146**: p. 215-224.
24. Yadav, K.K., et al., *Fluoride contamination, health problems and remediation methods in Asian groundwater: A comprehensive review*. 2019. **182**: p. 109362.

25. Lee, H., et al., *Emergence and spread of cephalosporin-resistant Neisseria gonorrhoeae with mosaic penA alleles, South Korea, 2012–2017*. 2019. **25**(3): p. 416.
26. Gleick, P.H. and M.J.P.o.t.N.A.o.S. Palaniappan, *Peak water limits to freshwater withdrawal and use*. 2010. **107**(25): p. 11155-11162.
27. Stumm-Zollinger, E. and G.M. Fair, *Biodegradation of steroid hormones*. Journal (Water Pollution Control Federation), 1965: p. 1506-1510.
28. Daughton, C.G. and T.A. Ternes, *Pharmaceuticals and personal care products in the environment: agents of subtle change?* Environmental health perspectives, 1999. **107**(suppl 6): p. 907-938.
29. Wu, C., et al., *Water pollution and human health in China*. 1999. **107**(4): p. 251-256.
30. Chander, V., et al., *Pharmaceutical compounds in drinking water*. 2016. **6**(1): p. 5774.
31. Kairigo, P., et al., *Contamination of surface water and river sediments by antibiotic and antiretroviral drug cocktails in low and middle-income countries: occurrence, risk and mitigation strategies*. 2020. **12**(5): p. 1376.
32. Almufarrij, R.S., et al., *Sweep-Out of Tigecycline, Chlortetracycline, Oxytetracycline, and Doxycycline from Water by Carbon Nanoparticles Derived from Tissue Waste*. Nanomaterials, 2022. **12**(20): p. 3617.
33. Topare, N.S. and S.A. Bokil, *Adsorption of textile industry effluent in a fixed bed column using activated carbon prepared from agro-waste materials*. Materials Today: Proceedings, 2021.
34. Yurtsever, A., et al., *Self-forming dynamic membrane bioreactor for textile industry wastewater treatment*. Science of The Total Environment, 2021. **751**: p. 141572.
35. Feng, Q., et al., *Flocculation performance of papermaking sludge-based flocculants in different dye wastewater treatment: Comparison with commercial lignin and coagulants*. Chemosphere, 2021. **262**: p. 128416.
36. Othman, M.H.D., et al., *Advanced Membrane Technology for Textile Wastewater Treatment*, in *Membrane Technology Enhancement for Environmental Protection and Sustainable Industrial Growth*. 2021, Springer. p. 91-108.
37. Chowdhury, M.F., et al., *Current treatment technologies and mechanisms for removal of indigo carmine dyes from wastewater: A review*. Journal of Molecular Liquids, 2020: p. 114061.
38. Harrache, Z., et al., *Thermodynamic and kinetics studies on adsorption of Indigo Carmine from aqueous solution by activated carbon*. Microchemical Journal, 2019. **144**: p. 180-189.
39. Oberoi, A.S., et al., *Insights into the fate and removal of antibiotics in engineered biological treatment systems: a critical review*. Environmental science & technology, 2019. **53**(13): p. 7234-7264.
40. Jones, O.A., J.N. Lester, and N.J.T.i.B. Voulvoulis, *Pharmaceuticals: a threat to drinking water?* 2005. **23**(4): p. 163-167.
41. Hussin, F., M.K. Aroua, and M.A.J.E. Kassim, *Transforming Plastic Waste into Porous Carbon for Capturing Carbon Dioxide: A Review*. 2021. **14**(24): p. 8421.